Two Novel Multiband Centimetre-Wave Patch Antennas for a Novel OFDM Based RFID System

Nayan Sarker[1], Md. Aminul Islam[2], and M. Rubaiyat Hossain Mondal[1]
[1] Institute of Information and Communication Technology (IICT), Bangladesh University of Engineering and Technology (BUET), Dhaka-1000, Bangladesh
[2] Department of Electrical, Electronic and Communication Engineering (EECE), Military Institute of Science and Technology (MIST), Mirpur Cantonment, Dhaka-1216, Bangladesh
Email: nayan_ece09@yahoo.com; aminul9274@gmail.com; rubaiyat97@yahoo.com

Abstract —Two novel multiband patch antennas operating at centimetre band are proposed for a novel orthogonal frequency division multiplexing (OFDM) based radio-frequency identification (RFID) reader. Here, the first one is a dual band antenna with centre frequencies of 7.30 GHz and 9.50 GHz, while the second one is a triple band antenna centred at 7.75 GHz, 9.70 GHz and 11.90 GHz. Both the patch antennas are designed with equal-width horizontal arms as radiating elements and a microstrip feeding line as the feeder. The antennas are moderately small sized with dimensions of 40.30 mm by 35.10 mm. Simulations with Computer Simulation Technology (CST) Microwave Studio tool indicate that competitive values of different antenna parameters are achieved when compared with centimetre band antennas described in the literature. With the use of MATLAB tool, the bit error rate (BER) performance of the multiband antennas are simulated for outdoor Rayleigh and Rician fading channels. Simulation results for the proposed two antennas indicate that for a given number of OFDM subcarriers, the larger the bandwidth of the signals received by the RFID reader, larger the BER degradation. These results have confirmed the usability of the designed antenna in commercial OFDM based RFID readers.

Index Terms—Bandwidth, Bit Error Rate (BER), centimetre-wave, multipath fading, Orthogonal Frequency Division Multiplexing (OFDM), patch antenna, Radio Frequency Identification (RFID).

I. Introduction

In recent years, radio-frequency identification (RFID) has become a promising technology in the field of object identification. A typical RFID system consists of a reader, a reader antenna, a host computer, middleware software for the computer, and tags attached on items. RFID uses electromagnetic fields to identify and track tags that store electronic information about objects they are attached to. RFID can read objects at a range up to 100 metres, can read considerable number of information at a time and can be usable for both outdoor and indoor environment. Unlike optical barcode systems, no-line-of sight (NLOS) communication is possible by RFID systems. RFID has several applications including library management, cattle identification, toll collection, flood level detection, parking access control, security, retail stock management, telemedicine and transportation logistic [1]-[3]. RFID also has potential applications in museums, art galleries, hospitals, and military. Various frequency bands are used worldwide for RFID such as High Frequency (HF), Ultrahigh Frequency (UHF), Super High Frequency (SHF) also known as centimetre wave band (3 GHz – 30 GHz), and millimetre wave band. Usually the design of the RFID antenna in any frequency band is a complex task. Because of wireless spectrum crunch, researchers are exploiting unused high frequencies in the centimetre band. Different countries of the world apply different frequencies for RFID communication. Moreover, different application scenarios within a country require different frequencies. So, there is a need of designing a single antenna having multiple resonance frequencies. For instance, having a dual band and triple band antenna allows these to be used in two or three different types of wireless application scenarios, respectively [4], [5].

An RFID signal in the outdoor environment may experience multipath fading or distortion. In the case of outdoor scenarios, Rayleigh or Rician fading and Doppler spread occurs [6]-[8]. These impairments cause inter symbol interference (ISI) as well as Inter Carrier Interference (ICI). Therefore, in the presence of these impairments, the overall bit error rate (BER) increases and the reading range suffers. Similar to 4G cellular communication scenarios, Orthogonal Frequency Division Multiplexing (OFDM) encoding technique may be used to combat multipath effects in outdoor RFID systems [9]-[14].

A number of research papers [15]-[22] report RFID systems where antennas operate in centimetre band. Furthermore, a number of antennas [23]-[27] studied for wireless applications can be adapted for RFID applications. One example of antenna designs for RFID applications is the work in [21] presenting an elliptical patch textile antenna at 2.45 GHz. A dual band tag antenna at 2.45 GHz and 5.8 GHz is proposed in [22]. A compact dual band antenna operating around the range of 2.4 GHz and 5.0 GHz is proposed for RFID systems in [18], [20]. The authors of [17] describe a dual band antenna at resonance frequencies of 2.44 GHz and 5.77 GHz, and a triple band antenna at resonance frequencies of 2.44 GHz, 3.55 GHz and 5.79 GHz. Similarly, the authors of [19] present high bandwidth high gain dual

Manuscript received January 27, 2018; revised May 18, 2018.
Corresponding author email: nayan_ece09@yahoo.com.
doi:10.12720/jcm.13.6.303-316

band and triple band antennas at 2.4 GHz and 5.8 GHz bands. Different designs of 10 GHz antennas are proposed for RFID scheme by the authors of [15]. Furthermore, a quasi-isotropic antenna at 10.5 GHz is devised for RFID tags in [16]. However, none of these works evaluate the BER performance of the RFID systems. Only the concept of OFDM based RFID system is proposed in [28]. However, a detail investigation of OFDM based RFID scheme and the evaluation of BER is yet to be done. In this paper, we focus on an OFDM based outdoor RFID system operating in the centimetre band. The contributions of this paper can be summarized as follows:

1) A dual band and a triple band antenna are proposed centred around 8 GHz - 12 GHz for RFID reader section. This new multiband design is adapted from the design of a single band 10 GHz antenna described in [15].
2) Based on the bandwidths of the proposed new antennas, the BER performance of the RFID communication system is evaluated for the case where the transmitted signal bandwidth is equal to the reader antenna bandwidth.
3) Comparisons are made between the proposed RFID antennas and the relevant antennas described in the literature.

The rest of the paper is organized as follows. In Section II, an OFDM based RFID system is described. The design of a dual and a triple band antenna is introduced in Section III. Simulation results on the bandwidths, gain, directivity, radiation efficiency, etc. for both antennas are presented in Section IV. Next, Section V presents the BER performance using designed antenna bandwidth, where the effects of fading channel (Rayleigh and Rician) are studied. In addition, a comparative study between dual and triple band antennas with various reference antennas is discussed in Section VI. Finally, Section VII provides concluding remarks.

II. OFDM Based RFID System Description

The block diagram of a complete RFID communication system is shown in Fig. 1. The main components of a RFID system are a RFID reader, RFID tags, antennas (both for reader and tag), a RFID middleware and destination host PC or a monitoring system. Generally, the RFID reader is known as interrogator that acts as a Radio Frequency (RF) transceiver. The RFID reader system is controlled by a Digital Signal Processor (DSP) or a microprocessor. The RFID tag contains an Integrated Circuit (IC) commonly known as microchip associated with an antenna. The tag is placed to an object to identify. Tags can be classified into two major categories depending on tag on board power supply which are active or passive tag [29]. If the tag has on board power supply then it is called active tag, otherwise it is called passive. Based on the Application Specific Integrated Circuits (ASIC) in tag (transponder) section, RFID systems can be categorized as chip based and chip less RFID.

First of all, the RFID reader antenna transmits energy signal as well as clock signal to the tag system. The tag antenna receives energy signal to power up the tag microchip. Then reader sends data signal to the tag. The tag antenna receives the reader signal and processes it. After processing, the tag microchip retransmits a backscatter signal associated with data signal to the reader. The backscatter signal is more strengthen if tag antenna's inductive impedance is perfectly matched with tag microchip capacitive impedance. Finally, the reader decodes tag backscatter signal and sends it to the destination host or central monitoring system via RFID middleware. It is notable that the read range of RFID system depends on several parameters such as either the tag is active or passive, reader and tag antenna gain, directivity, obstacles between reader and tag and the wireless channel overall. It has already been mentioned that in a practical outdoor wireless channel, multipath fading causes inter symbol and inter carrier interference to degrade the system performance. The use of OFDM waveform can combat this effect. Therefore, OFDM transmitter can be used at the tag section and OFDM receiver at the reader section. In the following, the OFDM transmitter and receiver useful in outdoor RFID system are described.

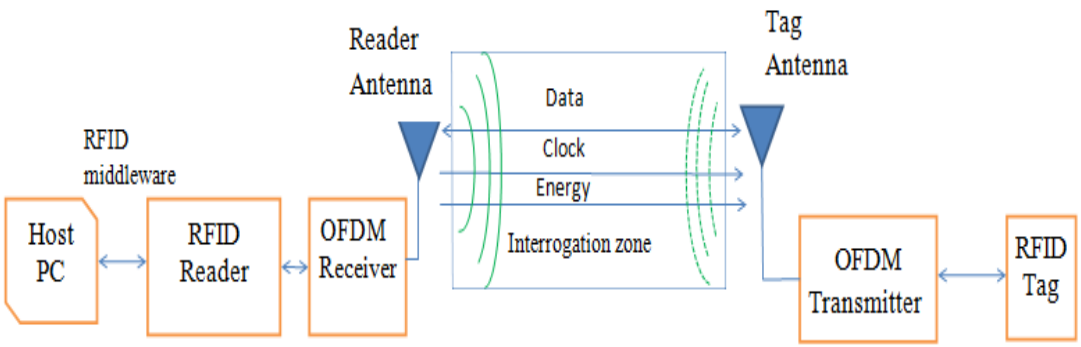

Fig. 1. Block diagram of an OFDM based RFID system.

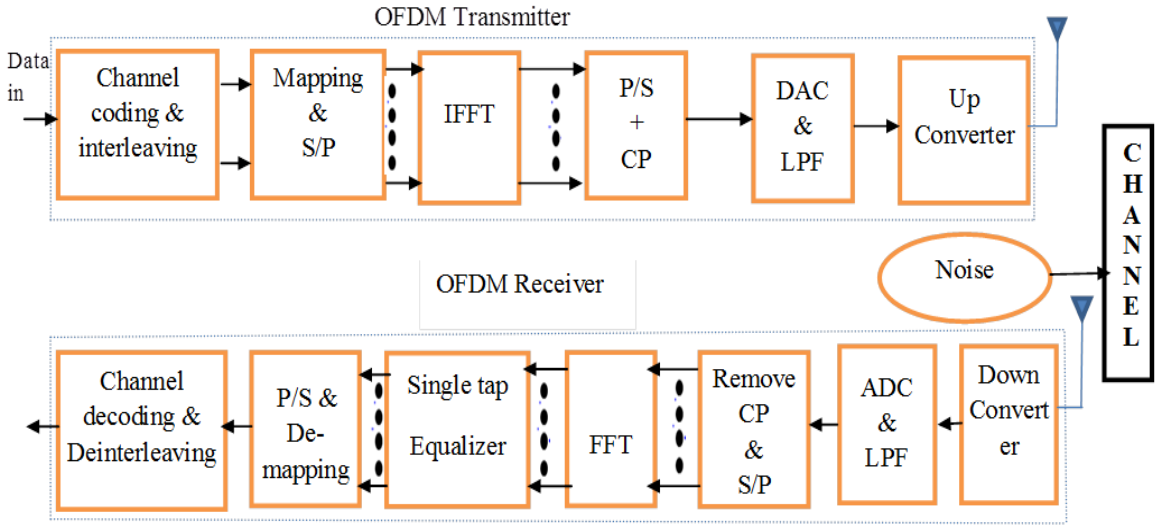

Fig. 2. Block diagram of an OFDM transmitter and receiver.

Fig. 2 shows the typical block diagram of an OFDM transmitter and receiver system [9]-[13]. At the OFDM transmitter, channel coding and interleaving are performed. High speed serial data streams are then mapped onto complex numbers from the constellation being used such as M-array pulse amplitude modulation (M-PAM), M-array quadrature amplitude modulation (M-QAM) or M-array phase shift keying (M-PSK). The complex constellations are converted into N number of lower speed parallel data streams using serial to parallel (S/P) conversion block. These parallel data streams are converted into time domain complex numbers from the frequency domain using N -point Inverse Fast Fourier Transform (IFFT) block. The complex time domain samples at the output of the IFFT are given by following expression

$$x(t) = \frac{1}{\sqrt{N}} \sum_{k=1-\frac{N}{2}}^{N/2} X_k \exp(\frac{j2\pi tk}{T})$$

$$\text{for} \quad 1-N/2 \le k \le N/2 \qquad (1)$$

where k is the subcarrier index, T is the symbol period before adding cyclic extensions, and the smaller case letters denote time domain and the upper-case letters denote frequency domain samples. After converting the parallel signals to serial sequence using parallel to serial (P/S) converter at the output of the IFFT, a cyclic extension known as Cyclic Prefix (CP) is added. By adding a CP, the symbol period is increased which is higher than the delay spread (δ) and thus minimizes multipath fading effects. A digital to analog converter (DAC) is then used to convert the samples of this extended OFDM symbol to continuous time domain analog signals and filtered by a low pass filter (LPF) to avoid unwanted signal frequency and finally are up-converted to the desired frequency before transmission [9]-[13].

At the OFDM receiver, the received signal is first down converted to base band signal. The base band signal is then converted to discrete signals by passing through a LPF and Analog to Digital Converter (ADC). The received discrete base band time domain signal is fed to an N -point FFT block after the removal of CP and the S/P conversion. The FFT output is described by the given equation

$$X_k = \frac{1}{\sqrt{N}} \sum_{t=1-N/2}^{N/2} x(t) \exp(-\frac{j2\pi kt}{T})$$

$$\text{for} \quad 1-N/2 \le t \quad t \le N/2 \qquad (2)$$

After that the FFT output is equalized to obtain the desired frequency domain signal by a single tap zero forcing equalizer. Finally, the original information is recovered by channel decoding and de-interleaving using the demodulation block [9]-[13].

III. Esign of Two Antennas in Centimetre band

Both the antennas are designed based on a single band microstrip antenna shown in [15]. Computer Simulation Technology (CST) Microwave Studio is used for antenna simulation and optimization. Commercially available Rogers RT5880 substrate with permittivity, ε_r = 2.2, loss tangent, $\tan\delta$ = 0.0009, substrate thickness, h = 0.787 mm, and copper thickness, t = 0.018 mm is used for the antenna design. The initial length and width of the two antennas are obtained by taking 10 GHz resonance frequency. In order to obtain the dual band and the triple band, the length and the width are adjusted to maximize the antenna performance. The detail design procedure is described in the next sections.

A. Dual Band Antenna Design

Plan view and 3-D perspective view of the dual band centimetre wave microstrip patch antenna are shown in Fig. 3. Here, the proposed dual band antenna is designed

and optimized with resonance frequencies f_{r1} = 7.30 GHz and f_{r2} = 9.50 GHz on Rogers RT5880 substrate. The optimized dimensional parameter values of the proposed dual band antenna are shown in Table I.

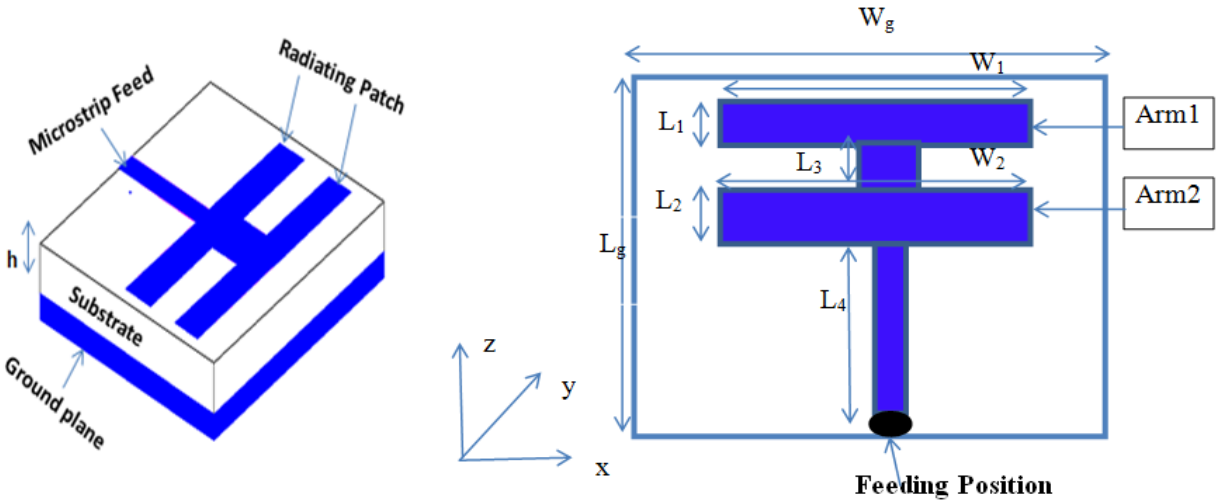

Fig. 3. A 3-D and a 2-D view of dual band RFID reader antenna.

TABLE I: SPECIFICATIONS OF DUAL BAND ANTENNA.

Antenna Parameters	Length in mm
W_g	40.29
L_g	35.12
$W_1 = W_2$	36.29
L_3	5
L_4	15.56
L_1	6.56
L_2	7
W_3 (Width of L_3)	7
W_4 (Width of L_4)	3

Here, two horizontal metal plates denoted as Arm1 and Arm2 with the same width ($W_1 = W_2$ =36.29 mm) are used as the main radiating element of the proposed dual band antenna. The length of radiator arms Arm1 (L_1) and Arm2 (L_2) are 6.56 mm and 7 mm, respectively. A single microstrip feeding line is used to feed this antenna so that it is comparable to an array of two extra wide microstrip patch elements [15]. The width and the length of radiator that connects Arm1 and Arm2 is W_3 =7 mm and L_3 =5 mm, and the width and the length of the microstrip feedline is W_4 = 3 mm and L_4 = 15.56 mm, respectively.

Finally, a copper ground is placed on the opposite side of the antenna substrate to complete the design. The length of the radiator that connects Arm1 and Arm2 is initially obtained using the procedure and expressions given in (3)-(4) [30]. In order to obtain the antenna's higher order transverse electromagnetic modes (TEM) whose attributes are very closely matched with the fundamental mode, a technique is introduced to calculate the proposed antenna's length and width. This technique is commonly known as size extension method [31]. According to the size extension method, the extended patch antenna width 'W' and length 'L' can be expressed as [31]:

$$W = \frac{(2N+1)}{\sqrt{(2\varepsilon_r+1)/2}} \times (\frac{\lambda}{2}) \tag{3}$$

$$L = \frac{(2N+1)}{\sqrt{\varepsilon_{eff}}} \times (\frac{\lambda}{2}) - 2\Delta L \tag{4}$$

where λ is the proposed antenna's operating wavelength, ε_r is the relative permittivity (dielectric constant) and N is a positive valued integer number (in this antenna design we assume N =1). Due to the fringing field effect, the physical dimensions of the microstrip patch antenna would look electrically wider. The extended length of the patch ΔL on each side is a function of antenna width to substrate height ratio (W/h) and the effective dielectric constant ε_{eff} [32]. So, ΔL and ε_{eff} are obtained by the following equations

$$\Delta L = 0.412h \frac{(\varepsilon_{eff}+0.3)(0.264+W/h)}{(\varepsilon_{eff}-0.3)(0.8+W/h)} \tag{5}$$

where effective dielectric constant,

$$\varepsilon_{eff} = \frac{\varepsilon_r+1}{2} + (\frac{\varepsilon_r-1}{2})(1+12\frac{h}{W})^{-\frac{1}{2}} \tag{6}$$

To feed the proposed antenna microstrip transmission line length, $L_4 = L_T$, and its input impedance Z_{in} are obtained by the expression introduce in [23]

$$Z_{in} = 29.9\frac{\lambda_0}{W} \quad (7)$$

$$L_T = \frac{(2M+1)}{2} \times (\frac{\lambda}{2}) \quad (8)$$

where M is assumed as a positive valued integer number (in the designed antenna M =1) and λ_0 is the operating wavelength at free space in desired frequency.

The equations described above are used to design a dual band (one band at frequency 7.30 GHz and other band at 9.50 GHz) linearly polarized antenna. Initially the transmission line length L_4 and width W_4 are obtained using equations given in [30]. The ground plane width and length '$W_g = W + 6h$' and '$L_g = L + 6h$' are initially set respectively from the method described in [15]. For better antenna performance, the length and width are adjusted using optimization tools of CST Microwave Studio. Using optimization tools of CST, the length of Arm2 is adjusted as L_2 =7 mm, and the lengths of connector Arm1 and Arm2 are adjusted to L_3 = 5 mm. Desired impedance matching, acceptable gain, directivity, resonance frequency at centimetre band, S_{11} parameters, Lowest Side Lobe Level (LSLL), radiation efficiency are achieved by final optimization using CST of the proposed dual band antenna for RFID reader applications.

B. Triple Band Antenna Design

By modifying the dual band antenna structure described in the previous section, a novel triple band antenna at centimetre band is designed in this section. Plan view of the triple band antenna design is shown in [33]. The design mechanism of the proposed triple band antenna at centimetre band with three resonance frequencies is almost similar to the dual band antenna which is described in Section III.A. The main difference between the proposed dual band and the triple band antenna is the number of horizontal arms as well as the variation in length of the horizontal arms. The length and the width of various radiator elements of triple band antenna are obtained by the same equations that are described in Section III. Three horizontal metal plates denoted as Arm1, Arm2, and Arm3 with the same width (W_1 = W_2 = W_3 = 36.30 mm) are used as the main radiator element of this proposed antenna. The lengths of Arm2 and Arm3 are the same, $L_2 = L_3$ = 5 mm, and the length of Amr1 is L_1 = 3 mm.

A single microstrip feeding line is used to feed this antenna so that it is comparable to an array of three extra wide microstrip patch elements. The length of radiator that connects Arm1 and Arm2 and the length of microstrip feedline is L_4 =5 mm and $L_T = L_6$ =10.12 mm, respectively. Better antenna performances are achieved by optimizing antenna's various parameters using optimization tools of CST Microwave Studio. The optimized dimensional parameters of the triple band antenna are shown in tabular form in Table II.

TABLE II: SPECIFICATIONS OF TRIPLE BAND ANTENNA.

Antenna parameters	Length in mm
W_g	40.29
L_g	35.12
W_1=W_2=W_3	36.30
L_4=L_5	5
L_6	10.12
L_1	3
L_2=L_3	5
W_4 (Width of L_4)	5
W_5 (Width of L_5)	8
W_6 (Width of L_6)	4

IV. SIMULATION RESULTS OF THE ANTENNA PERFORMANCE

The simulation results of the optimized dual band and triple band microstrip patch antennas (Fig. 4) for OFDM based RFID reader using CST Microwave Studio are described in the next sections.

A. Simulation Results of the Optimized Dual Band Antenna

The simulation results of the proposed dual band antenna using waveguide ports are at resonance frequencies f_{r1} = 7.30 GHz and f_{r2} = 9.50 GHz are presented in this section. The simulated return loss at f_{r1} is 32.25 dB and at f_{r2} is 41.0 dB, which are shown in Fig. 5. This indicates antenna impedance is considerably matched with the waveguide port impedance as less amount of power is reflected back from the input terminal of the antenna.

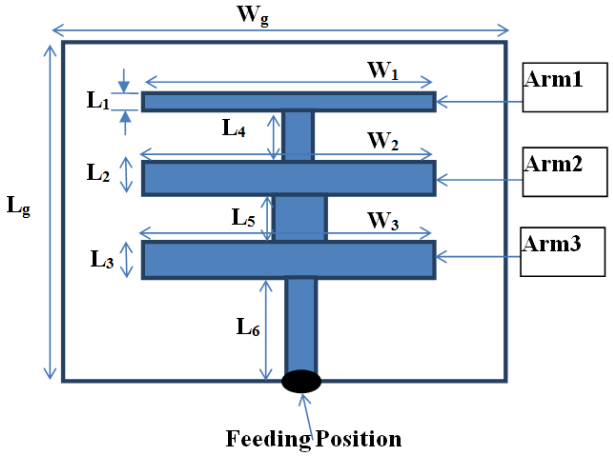

Fig. 4. Triple band RFID reader antenna.

Fig. 5 and Fig. 7 show the simulated E-plane (φ=0^0) and H-plane ((φ=90^0) far field radiation patterns at f_{r1} and f_{r2}, respectively indicating side lobe level, 3 dB angular beam width, main lobe magnitude and main lobe direction. It can be seen from Fig. 6 and Fig. 7 that the side lobe levels at both resonance frequencies are above -

13dB which ensures that maximum power is concentrated at main lobe so that tag antenna receives more power from the reader. The gain versus frequency plots, and the radiation efficiency versus frequency curves of this dual band antenna are shown in Fig. 8 and Fig. 9, respectively.

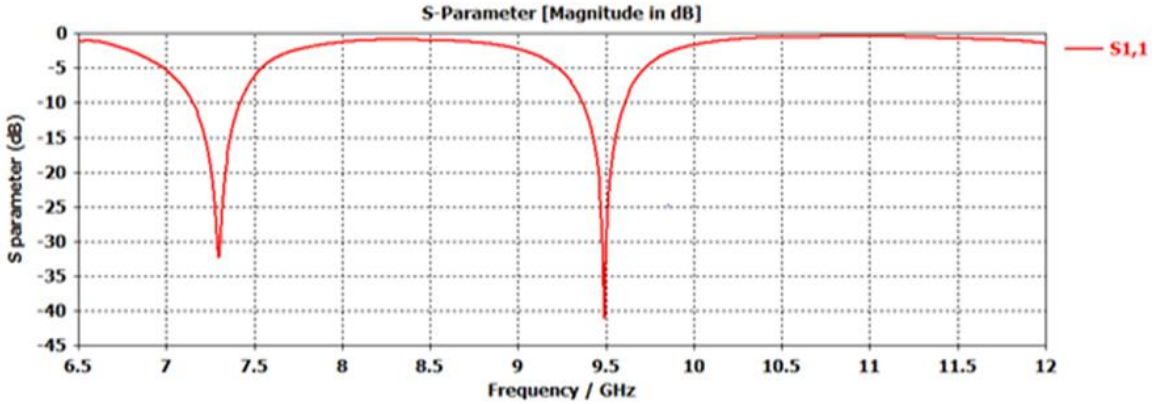

Fig. 5. Reflection co-efficient (S11) of the dual band reader antenna.

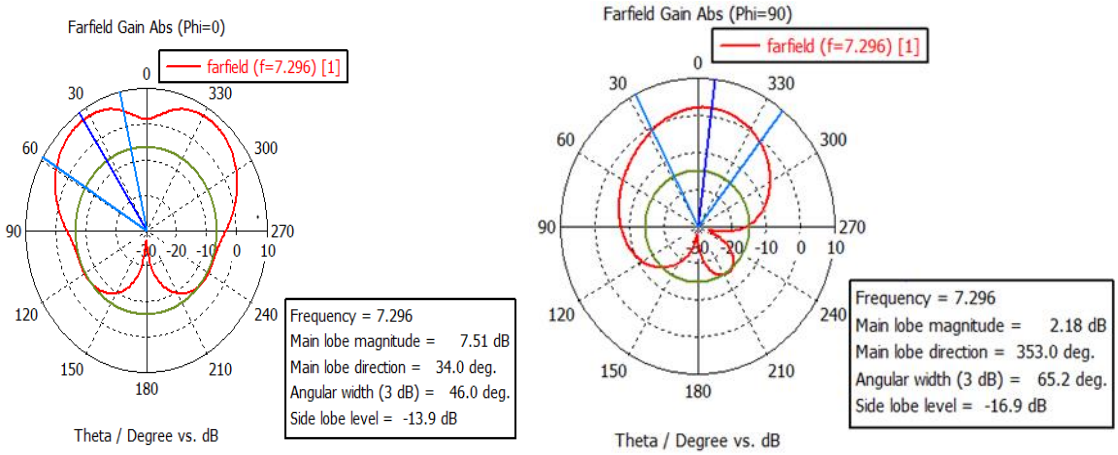

Fig. 6. E and H-plane radiation pattern for dual band reader antenna at f_{r1} = 7.30 GHz.

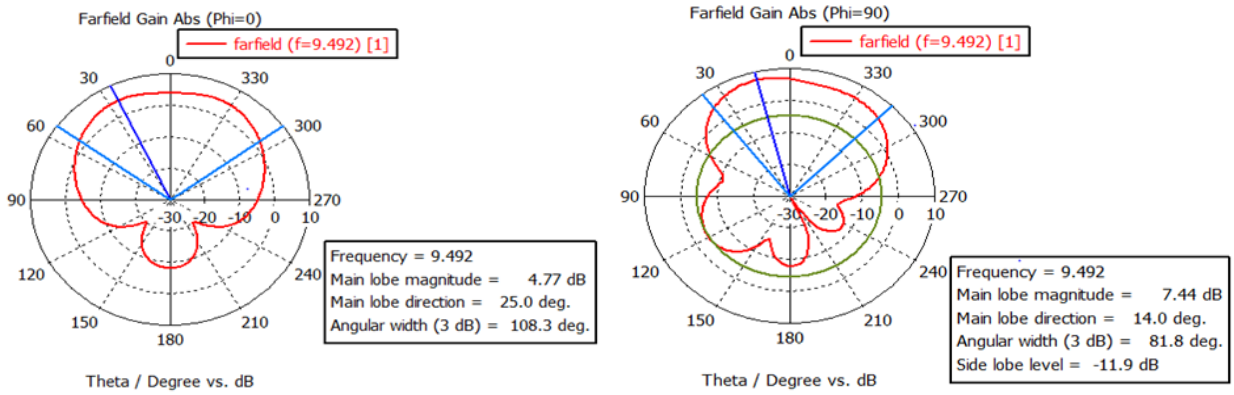

Fig. 7. E and H-plane radiation pattern for dual band reader antenna at f_{r2} = 9.50 GHz

It can be seen from Fig. 8 and Fig. 9 that gain at resonance frequency f_{r1} is slightly higher than the gain at resonance frequency f_{r2} , but the radiation efficiency at both of the resonance frequencies is almost same. The antenna gain (G) and directivity (D) at f_{r1} are 7.628 dB and 8.339 dBi, respectively. Moreover, the antenna gain and directivity at f_{r2} are 5.60 dB and 6.198 dBi, respectively. The antenna radiation efficiency is related to the gain and directivity and it can be written as $\eta = G(dB) - D(dB)$. So, the antenna radiation efficiency at 7.30 GHz is 85.00% and at resonance frequency of 9.50 GHz is 87.14%. The reflection coefficient curves in Fig. 5 show that the -10dB bandwidth at resonance f_{r1} is 300 MHz (4.11% of resonance frequency) ranging from 7.138 GHz to 7.438

GHz. The bandwidth decreases to 270 MHz (2.85% of resonance frequency) at f_{r2} ranging from 9.354 GHz to 9.624 GHz.

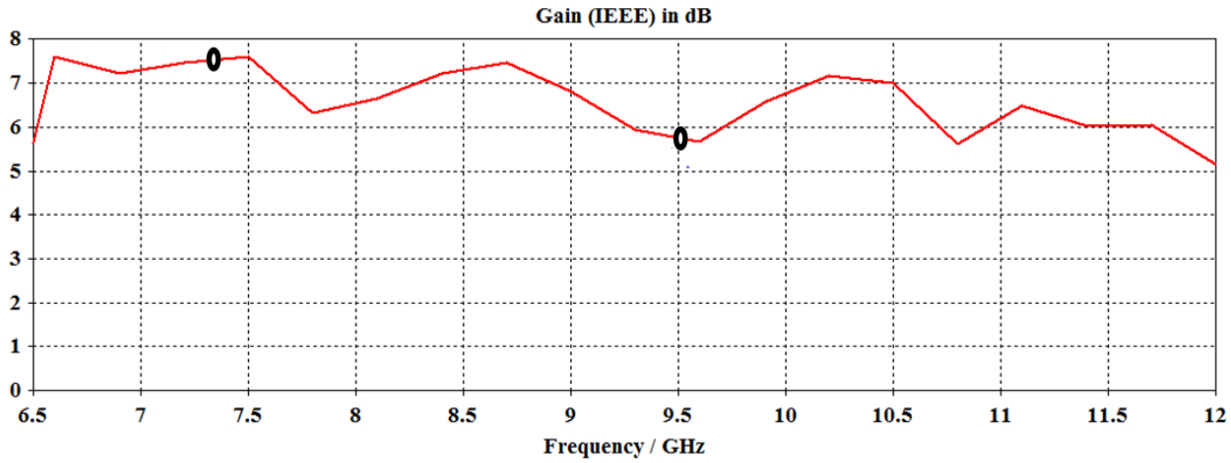

Fig. 8. Gain vs frequency for dual band reader antenna.

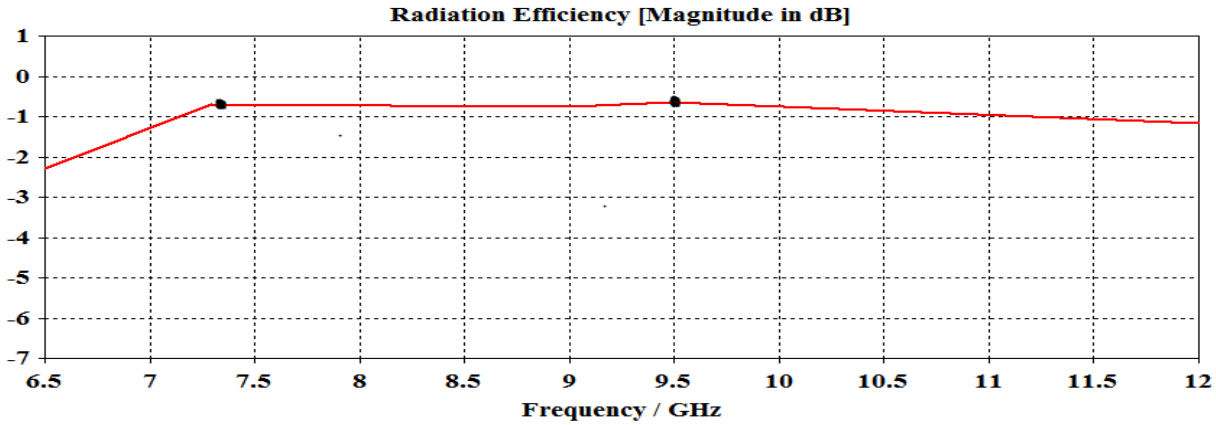

Fig. 9. Radiation efficiency for dual band reader antenna.

B. Parametric Study for the Dual Band Antenna

The effects of length variation of Arm2 (denoted as L_2) and the length of the vertical line (denoted as L_3) that connects horizontal Arm1 and Arm2 on the simulation result are observed. Due to the variation of lengths of L_2 and L_3, both the resonance frequencies of the proposed dual band antenna are changed. The effects of width variations are shown in Table III. Table III shows the variation of lengths L_2 and L_3, and corresponding effects on S-parameter, and resonance frequencies. The overall impact on S-parameter, and radiation effenciency are shown in Fig. 10 (a), and Fig. 10 (b), respectively. Table III indicates that when L_2 decreases and L_3 increases, the S-parameter increases, which means the antenna performance degrades. For all of the cases, the values of VSWR at both resonance frequencies are less than 1.50 which indicates that the antenna impedance is resonably matched with the waveguide port impedance. The best result is achieved when L_2 =7 mm and L_3 =5 mm, at which S_{11} =-32.25 and -41.011 for f_{r1} and f_{r2} respectively.

C. Simulation Results of the Optimized Triple Band Antenna

This designed antenna provides resonance at three separate frequency bands. The antenna dimensional parameters are almost similar to the dual band antenna discussed in the previous section except that the horizontal radiator width that is introduced in Section III-B. Various simulation results including return loss (S_{11}), radiation pattern (both E and H field) and gain versus frequency curves are shown in this section.

Fig. 11 shows the reflection co-efficient (S11) of the triple band reader antenna. Furthermore, Fig. 12, Fig. 13 and Fig. 14 show the radiation patterns of the antenna at f_{r1}, f_{r2} and f_{r3}, respectively. The simulated radiation pattern at every resonance frequency band shows the main lobe magnitude, 3 dB angular beam width, LSLL, and main lobe direction. The lowest side lobe level is -12 dB achieved at f_{r1}. The gain and directivity at three resonance frequencies are: 5.79 dB and 6.04 dBi, 6.67 dB and 7.09 dBi, and 3.88 dB and 4.33dBi at f_{r1}, f_{r2} and f_{r3}, respectively. So, the radiation efficiency of this triple band proposed antenna are 94.34%, 90.88% and

90.09% at f_{r1}, f_{r2} and f_{r3}, respectively. The -10 dB return loss bandwidth at these three resonance frequencies are 180 MHz (2.33% of resonance frequency) ranging from 7.66 GHz to 7.84 GHz, 177 MHz (1.83% of resonance frequency) ranging from 9.63 GHz to 9.80 GHz, and 587 MHz (4.93% of resonance frequency) ranging from 11.630 GHz to 12.217 GHz.

TABLE III: SPECIFICATIONS OF DUAL BAND ANTENNA WITH VARIATION IN WIDTH.

SL No.	Arm2 (L_2 in mm)	L_3 in mm	Resonance frequency GHz		S-parameter S_{11} in dB		Radiation Efficiency (η_{rad})	
			f_{r1}	f_{r2}	S_{11} at f_{r1}	S_{11} at f_{r2}	η_{rad} (%) at f_{r1}	η_{rad} (%) at f_{r2}
i.	7	5	7.30	9.50	-32.250	-41.011	85.00	87.14
ii.	5	7	7.245	9.46	-22.129	-25.435	84.14	83.17
iii.	3	9	7.185	9.48	-14.770	-20.348	80.16	81.85
iv.	9	3	7.316	9.58	-20.826	-22.055	85.31	86.00

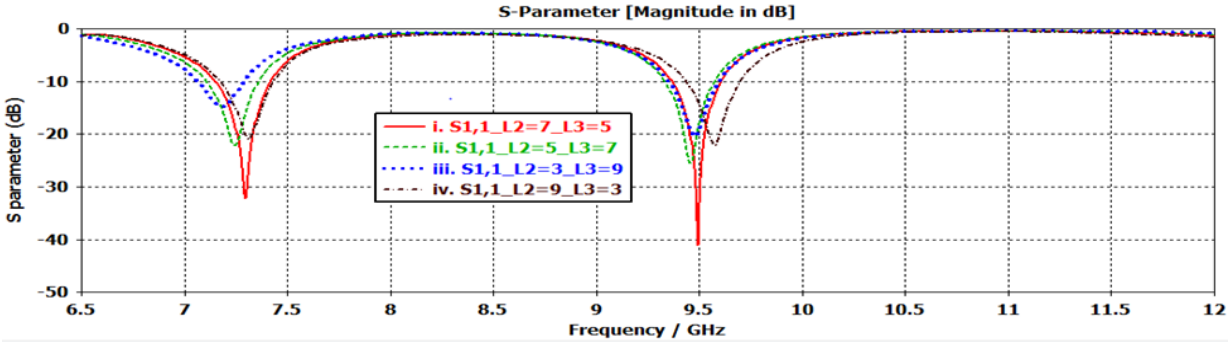

(a)

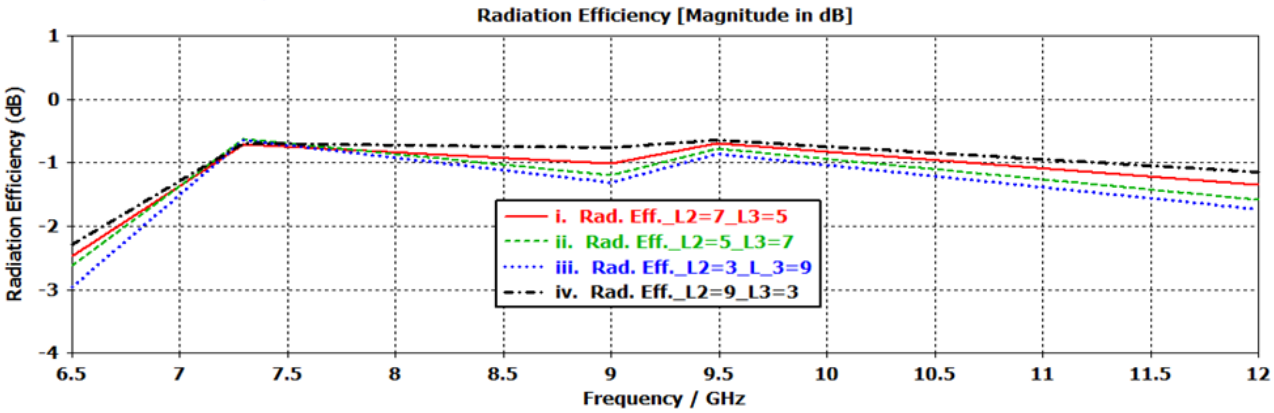

(b)

Fig. 10. Effects of length variation of L_2 and L_3 on S-parameter, and Radiation efficiency are shown in (a) and (b) respectively.

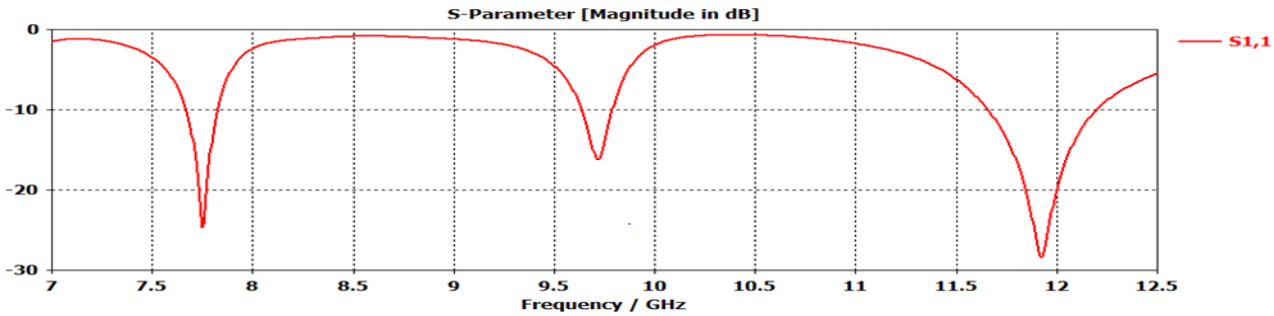

Fig. 11. Reflection co-efficient (S11) of the triple band reader antenna.

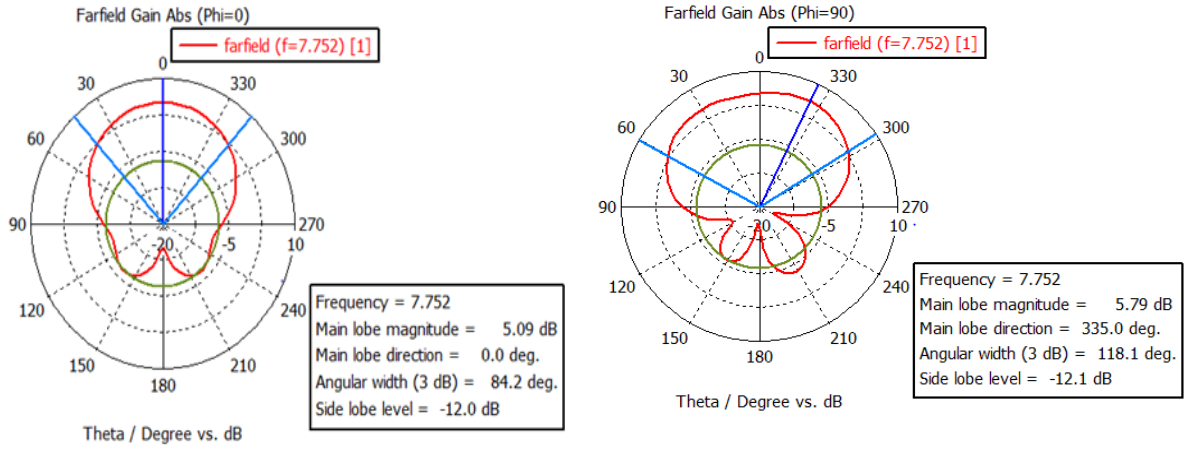

Fig. 12. E and H-plane radiation pattern for triple band reader antenna at f_{r1} =7.75 GHz.

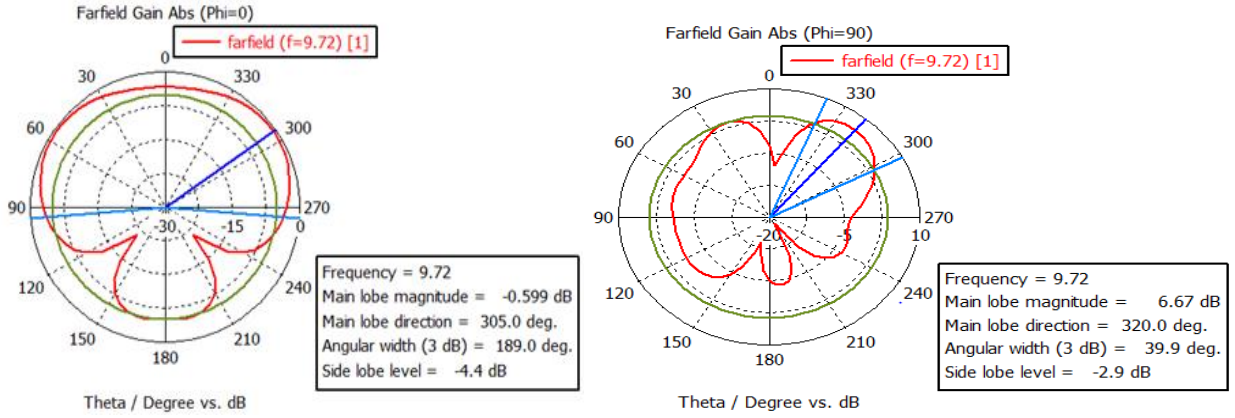

Fig. 13. E and H-plane radiation pattern for triple band reader antenna f_{r2} =9.72 GHz.

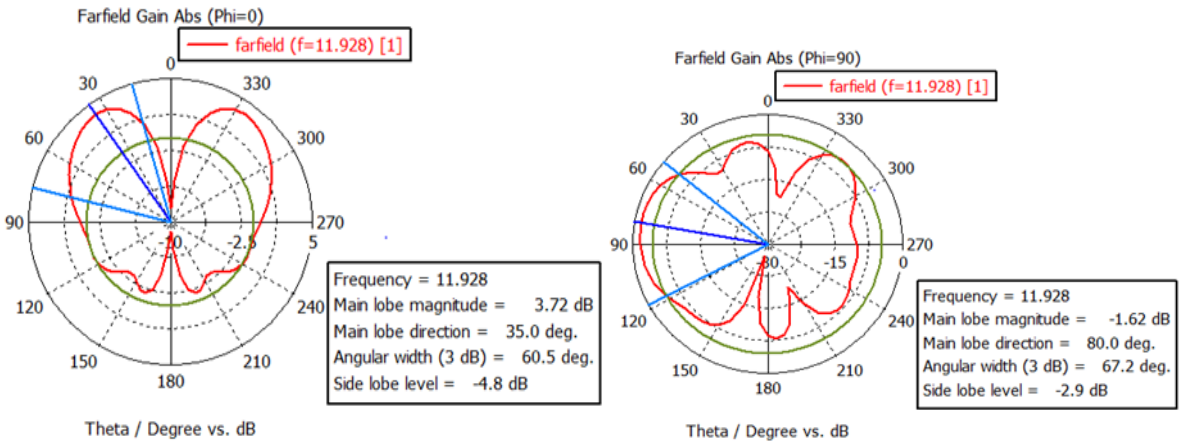

Fig. 14. E and H-plane radiation pattern for triple band reader antenna at f_{r3} =11.93 GHz.

V. BER Performance of the Proposed Antennas in the Centimetre Band

In this section, the BER performance of an RFID system is simulated via MATLAB tool. The detail simulation parameters are shown in Table IV. The practical RFID system at outdoor may suffer many environmental effects such as multipath Rayleigh or Rician fading, Doppler spread (f_d) due to the relative motion of the object with respect to RFID reader along with path loss. It has been mentioned in the Introduction Section that OFDM is applied in this research to reduce the effects of multipath fading that exists in outdoor scenarios. In order to evaluate the BER performance for OFDM based RFID systems, the bandwidths of the transmitted signals are considered. It can be noted that the

total bandwidth of the signal is divided into the OFDM subcarriers. The OFDM symbol duration which is the reciprocal of the bandwidth of a subcarrier should be greater than the channel delay spreads (σ). Therefore, the BER performance is a function of the bandwidth of each subcarrier [10]-[13]. An antenna with a large bandwidth can effectively receive a signal of the same bandwidth. In the following, we consider that the transmitted signal bandwidth is equal to the reader antenna bandwidth. Due to multipath fading, the power received by receiving antennas through line of sight (LOS) and non-line of sight components (N-LOS) are different and corresponding σ are also different. We consider single tap zero forcing equalizer at the RFID reader section. In the simulations, an uncoded target BER of 10^{-4} is considered. This target BER of 10^{-4} is approximately equivalent to 10^{-9} when channel coding is applied.

TABLE IV: PARAMETERS FOR BER SIMULATIONS

Parameters	**Quantity/Level**
Fading Channel	Rayleigh/ Rician
Baseband Modulation	QAM
Constellation Points	4, 16
Subcarrier Number	128, 256
Cyclic Prefix (CP)	25%
Doppler Spread (f_d)	100 Hz
Delay Spread (δ)	0.005×10^{-12} Sec
Antenna Bandwidth (Triple Band)	180 MHz, 177 MHz, 587 MHz.
Antenna Bandwidth (Dual Band)	270 MHz, 300 MHz

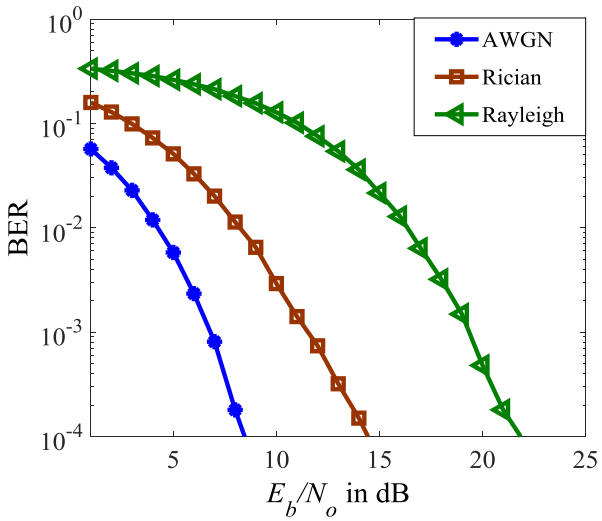

Fig. 15. BER performance of different channels at fixed bandwidth 270 MHz.

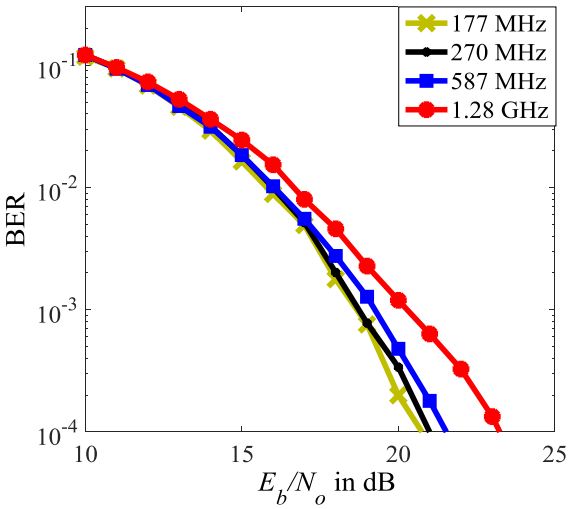

Fig. 16. BER performance at different resonance frequencies of the proposed antennas.

Fig. 15 represents the BER as a function of E_b/N_0, the received electrical energy per bit to single sided noise spectral density for the dual band antenna at f_{r2}. At f_{r2} the antenna bandwidth is 270 MHz, so the transmitted and the received signal bandwidths are also assumed to be 270 MHz. It can be seen that for both Rayleigh and Rician fading channels, E_b/N_0 penalty is occured in comparison with AWGN channels. In case of no fading (i.e. AWGN channel), E_b/N_0 of 8 dB is required to achieve a BER of 10^{-4}. The E_b/N_0 requirement for Rician fading channel is 14 dB and for Ralayeigh fading channel is 24 dB at a given BER of 10^{-4}. So, an extra 10 dB level of E_b/N_0 is required for Rayleigh fading than Rician fading, since in Rician fading a LOS path exsists between RFID reader and the tag. In comparison to AWGN channels, at a fixed BER of 10^{-4}, aditional 6 dB and 16 dB E_b/N_0 are needed for Rician and Rayleigh fading channels, respectively.

Fig. 16 shows the BER as a function of E_b/N_0 by using the bandwidths (177/270/587 MHz) of the proposed antennas and the bandwidth (1.28 GHz) of the antenna in [15]. It is seen that due to the variations of the antenna bandwidths (also the transmitted/received signal bandwidths), the E_b/N_0 requirement is varied for the same target BER. The graph presents that the E_b/N_0 requirement increases when bandwidth of the transmitted/received signal (per subcarrier) increases. For the same BER (10^{-4}), the E_b/N_0 requirements for bandwidth 177 MHz and 587 MHz are 20.8 dB and 21.5 dB, respectively. So, for a bandwidth 587 MHz, approximately 0.7 dB more E_b/N_0 is required than a bandwidth of 177 MHz. This is because as the bandwidth is lower, the symbol period is greater which means that the delay spread has less influence. Fig. 16 also shows that the BER performance is 1.8 dB better for a signal bandwidth of 587 MHz (equal to the bandwidth of the proposed triple band antenna) compared to a signal bandwidth of approximately 1.28 GHz which is equal to the bandwidth of the antenna proposed in [15].

VI. Comparative Study of Antennas

In both of the proposed dual band and triple band antennas, the S_{11} is always less than -10 dB at the resonance frequencies, which indicates that the designed antenna impedance is considerably matched with waveguide port impedance. In case of dual band antenna, the bandwidth at f_{r1} =7.30 GHz is 300 MHz which is slightly higher than the bandwidth of 270 MHz at f_{r2} =9.50 GHz. At f_{r1}, the S-parameter is -32.25 dB, whereas at f_{r2}, the value of S-parameter is -41.01 dB. The Lowest Side Lobe Level (LSLL) at H-plane for f_{r1} and f_{r2} are -16.90 dB and -11.90 dB, respectively. The radiation efficiency values for dual band antenna are 85.00% and 87.14% for f_{r1} and f_{r2}, respectively. Although large bandwidth is more desirable for antennas, a smaller bandwidth means more robustness to multipath fading effects. So, in terms of BER performance, radiation efficiency and S-parameters, f_{r2} is more preferable than f_{r1} for RFID communication in outdoor applications. In case of triple band antenna, the bandwidths at the three resonance frequencies (f_{r1}, f_{r2} and f_{r3}) are 180 MHz, 177 MHz and 587 MHz, respectively. The S-parameter and radiation efficiency levels at f_{r1} are -25.99 dB, and 94.34%, respectively. On the other hand, the S-parameter and radiation efficiency levels at f_{r2} are -15.85 dB and 90.88%, respectively. These two parameters have values of -29.34 dB and 90.09%, respectively at f_{r3}. The LSLL of the proposed triple band antenna at f_{r1}, f_{r2} and f_{r3} are -12.1 dB, -2.9 dB and -2.9 dB, respectively. The LSLL for dual band antenna at f_{r1} is -13.90 dB and -16.90 dB for E and H-plane, respectively. However, for triple band antenna, the LSLL at f_{r1} is -12.0 dB and -12.1dB for E and H-plane, respectively. So, the LSLL values are less in dual band compared to triple band where the lowest side lobe level indicates that maximum power radiates through the main lobe.

TABLE V: PERFORMANCE METRICS OF DUAL AND TRIPLE BAND ANTENNAS

Antennas		**Dual Band**		**Triple Band**		
Resonant Frequency (GHz)		f_{r1} =7.30	f_{r2} =9.50	f_{r1} =7.75	f_{r2} =9.72	f_{r3} =11.93
S-parameters (dB)		-32.25	-41.01	-25.99	-15.85	-29.34
Bandwidth		300.00	270.25	184.50	177.75	587.00
Rad. Efficiency (%)		85.00	87.14	94.34	90.88	90.09
Gain (dB)		7.628	5.06	5.793	6.674	3.882
Directivity (dBi)		8.339	6.198	6.046	7.089	4.335
Main lobe magnitude (dB)	**E-plane**	7.51	4.77	5.09	-0.599	3.72
	H-plane	2.18	7.44	5.79	6.67	-1.62
LSLL (dB)	**E-plane**	-13.90	-10.5	-12.0	-4.4	-4.8
	H-plane	-16.90	-11.9	-12.1	-2.9	-2.9
SNR requirement (dB) to achieve 10^{-4} BER		21.70	21.0	20.85	20.8	21.5

TABLE VI: COMPARISON OF THE PROPOSED ANTENNAS WITH THE LITERATURE.

Antenna	Size in mm^2	Operating Bands in GHz	Bandwidth in GHz	Gain (dB)
Ref [5]	100×70	0.915, 2.45	-	-
Ref [8]	43×36	10.00	0.29-1.28	13.05, 13.53, 13.64, 13.90
Ref [13]	120×40	2.40, 5.20, 5.80	0.51, 1.01	1.48, 2.30, 3.05
Ref [14]	34.35×29.52	10, 60	0.384	12.84
Ref [15]	52×37	10.5	1.575	3.08
Ref [16]	64×62	2.44 and 5.77	0.014, 0.349	4.96, 7.57
Ref [21]	13×12	2.98, 4.73, 5.70	-	2.59, 3.58, 2.29
Ref [23]	27.5×13	2.40, 3.50, 5.50	-	0.71, .95, 2.36
Ref [25]	100×60	2.4, 5.00	0.12, 2.10	8, 9
Ref [26]	130×130	0.922	0.106	4.9
Proposed Dual Band	40.30× 35.10	7.30, 9.50	0.27, 0.30	5.50, 7.628
Proposed Triple Band	40.30 × 35.10	7.75, 9.72, 11.93	0.185, 0.177, 0.587	5.793, 6.674, 3.882

In this section, the proposed dual and triple band antennas are compared with the antennas described in the relevant literature. An important feature of the proposed dual band and triple band antennas is that the sizes of the designed antennas are smaller than the antennas reported in [5], [15]-[18], [34]-[36]. However, the proposed dual and triple band antenna sizes are larger than the antennas reported in [37], [38] where the centre frequencies are less than those of the proposed antennas. Table VI shows that the gain values of the proposed antennas are higher than those of the reference antennas except the work in [15], [17], [18]. Table V also shows that triple band antenna has a resonance frequency at 11.93 GHz which is larger than any frequency described in [15]-[18], [34], [35], [37]. This makes the proposed triple band antenna attractive since RFID technology is moving towards centimetre and millimetre wave band [39] to solve the problem of the spectrum crunch. It can also be noted that, both the dual and triple band antennas have bandwidths lesser than the ones reported in [15], [16]. However, it has been shown in Section V that bit error increases when the received signal bandwidth increases in a multipath fading channel.

VII. CONCLUSION

Two multiband antennas with centre frequencies in the centimetre band are proposed in this paper. It is observed from simulations that the best values of gain, directivity, main lobe magnitude and the lowest side lobe level are obtained by the dual band antenna with a centre frequency of 7.3 GHz. On the other hand, the largest antenna bandwidth of 587 MHz is obtained by the triple band antenna with a centre frequency of 11.93 GHz. Simulation results also show that when the signal bandwidth received by the reader antenna increases from 177 MHz to 587 MHz, the BER performance degrades by 0.8 dB at an uncoded BER of 10^{-4}. Compared with the recent research reported in the literature, the multiband antennas are shown to have better gain operating at higher spectrum, without significantly increasing the physical dimensions. Experimental measurements of the proposed antennas are left for future work.

ACKNOWLEDGMENT

A portion of this work is a part of M.Sc. thesis of the author Nayan Sarker under the supervision of the author M. Rubaiyat Hossain Mondal to be submitted to the Institute of Information and Communication Technology (IICT) of Bangladesh University of Engineering and Technology (BUET).

REFERENCES

[1] K. Finkenzeller, *RFID Handbook: Radio-Frequency Identification Fundamentals and Applications*, John Wiley& Sons, 2000.

[2] R. Want, "An introduction to RFID technology," *IEEE Pervasive Computing*, vol. 5, pp. 25-33, 2006.

[3] S. B. Miles, S. E. Sharma, and J. R. Williams, *RFID Technology & Applications*, New York: Cambridge University Press 2011.

[4] C. Varadhan, J. K. Pakkathillam, M. Kanagasabai, R. Sivasamy, R. Natarajan, and S. K. Palaniswamy, "Triband antenna structures for RFID systems deploying fractal geometry," *IEEE Antennas and Wireless Propagation Letters*, vol. 12, pp. 437-440, 2013.

[5] A. K. Evizal, T. A. Rahman, S. K. B. A. Rahim, and M. F. B. Jamlos, "A multi band mini printed omni directional antenna with v-shaped for RFID applications," *Progress in Electromagnetics Research B*, vol. 27, pp. 385-399, 2011.

[6] K. Daeyoung, M. A. Ingram, and W. W. Smith, "Measurements of small-scale fading and path loss for

long range RF tags," *IEEE Transactions on Antennas and Propagation*, vol. 51, pp. 1740-1749, 2003.

[7] J. D. Griffin and G. D. Durgin, "Complete link budgets for backscatter-radio and RFID systems," *IEEE Antennas and Propagation Magazine*, vol. 51, pp. 11-25, 2009.

[8] A. Lazaro, D. Girbau, and D. Salinas, "Radio link budgets for UHF RFID on multipath environments," *IEEE Transactions on Antennas and Propagation*, vol. 57, pp. 1241-1251, 2009.

[9] G. E. B. a. T. C. P. Dent, *Jakes Fading Model Revisited*, Vol. 29, pp. 1162-1163, 1993.

[10] L. Hanzo, Y. Akhtman, L. Wang, and M. Jiang, *MIMO-OFDM for LTE, WiFi and WiMAX: Coherent Versus Non-Coherent and Cooperative Turbo Transceivers*, John Wiley & Sons Ltd., Oct. 2010.

[11] M. R. H. Mondal and S. P. Majumder, "Analytical performance evaluation of space time coded MIMO OFDM systems impaired by fading and timing jitter," *Journal of Communications*, vol. 4, pp. 380-387, 2009.

[12] A. Loulou and M. Renfors, "Enhanced OFDM for fragmented spectrum use in 5G systems," *Transactions on Emerging Telecommunications Technologies*, pp. 31-45, 2015.

[13] B. Farhang-Boroujeny, "OFDM versus filter bank multicarrier," *IEEE Signal Processing Magazine*, vol. 28, pp. 92-112, 2011.

[14] M. M. H. Mishu and M. R. H. Mondal, "Effectiveness of filter bank multicarrier modulation for 5G wireless communications," in *Proc. 4th International Conference on Advances in Electrical Engineering*, 2017, pp. 319-324.

[15] M. S. Rabbani and H. Ghafouri-Shiraz, "Improvement of microstrip patch antenna gain and bandwidth at 60 GHz and X bands for wireless applications," *IET Microwaves, Antennas & Propagation*, vol. 10, pp. 1167-1173, 2016.

[16] L. Pazin, A. Dyskin, and Y. Leviatan, "Quasi-Isotropic X-band Inverted-F antenna for active RFID tags," *IEEE Antennas and Wireless Propagation Letters*, vol. 8, pp. 27-29, 2009.

[17] L. Peng, C. L. Ruan, and X. H. Wu, "Design and operation of dual/triple-band asymmetric m-shaped microstrip patch antennas," *IEEE Antennas and Wireless Propagation Letters*, vol. 9, pp. 1069-1072, 2010.

[18] X. Quan, R. Li, Y. Cui, and M. M. Tentzeris, "Analysis and design of a compact dual-band directional antenna," *IEEE Antennas and Wireless Propagation Letters*, vol. 11, pp. 547-550, 2012.

[19] X. Liu, Y. Liu, and M. M. Tentzeris, "A novel circularly polarized antenna with coin-shaped patches and a ring-shaped strip for worldwide UHF RFID applications," *IEEE Antennas and Wireless Propagation Letters*, vol. 14, pp. 707-710, 2015.

[20] D. Najeeb, D. Hassan, R. Najeeb, and H. Ademgil, "Design and simulation of wideband Microstrip patch antenna for RFID applications," in *Proc. HONET-ICT*, 2016, pp. 84-87.

[21] S. H. Shehab, S. Hassan, M. A. I. Oni, S. Dey, and M. M. Hassan, "Design and evaluation of an elliptical patch textile antenna for RFID application and bending consequences," in *Proc. International Conference on Electrical Engineering and Information Communication Technology*, 2015, pp. 1-4.

[22] Y. Yu, J. Ni, and Z. Xu, "Dual-Band dipole antenna for 2.45 GHz and 5.8 GHz RFID tag application," *International Journal of Wireless Communications and Mobile Computing*, vol. 3, pp. 1-6, 2015.

[23] S. Genovesi, A. Monorchio, and S. Saponara, "Compact triple-frequency antenna for Sub-GHz wireless communications," *IEEE Antennas and Wireless Propagation Letters*, vol. 11, pp. 14-17, 2012.

[24] Y. He, K. Ma, N. Yan, and H. Zhang, "Dual-Band monopole antenna using substrate-integrated suspended line technology for WLAN application," *IEEE Antennas and Wireless Propagation Letters*, vol. 16, pp. 2776-2779, 2017.

[25] A. K. Gautam, L. Kumar, B. K. Kanaujia, and K. Rambabu, "Design of compact f-shaped slot triple-band antenna for WLAN/WiMAX applications," *IEEE Transactions on Antennas and Propagation*, vol. 64, pp. 1101-1105, 2016.

[26] A. K. Sharma, A. Mittal, and B. V. R. Reddy, "Slot embedded dual-band patch antenna for WLAN and WiMAX applications," *Electronics Letters*, vol. 51, pp. 608-609, 2015.

[27] L. Peng, Y. J. Qiu, L. Y. Luo, and X. Jiang, "Bandwidth enhanced l-shaped patch antenna with parasitic element for 5.8-GHz wireless local area network applications," *Wireless Personal Communications*, vol. 91, pp. 1163-1170, December 01 2016.

[28] S. P. Majumder and K. Mahmud, "Evaluation of detection range of an active RFID in outdoor environment using receiver diversity with maximal ratio combining," *International Journal of Information and Electronics Engineering*, vol. 5, pp. 322-329, 2015.

[29] D. M. Dobkin, *The RF in RFID: UHF RFID in Practice*, Second Edition ed. vol. 167, 2004.

[30] J. S. G. Hong and M. J. Lancaster, *Microstrip Filters for RF/Microwave Applications*, John Wiley & Sons, 2004 vol. 167.

[31] S. Szott and M. Natkaniec, "Emerging technologies in wireless LANs: Theory, design, and deployment (Bing, B., Ed.; 2008)," *IEEE Communications Magazine*, vol. 47, pp. 18-18, 2009.

[32] C. A. Balanis, *Antenna Theory: Analysis and Design*, 3rd Edition ed.

[33] D. Pozar, *M. Microwave Engineering*, John Wiley & Sons, 2009.

[34] C. M. Wu, C. N. Chiu, and C. K. Hsu, "A new nonuniform meandered and fork-type grounded antenna for triple-band WLAN applications," *IEEE Antennas and Wireless Propagation Letters*, vol. 5, pp. 346-348, 2006.

[35] C. K. Hsu and S. J. Chung, "Compact multiband antenna for handsets with a conducting edge," *IEEE Transactions on Antennas and Propagation*, vol. 63, pp. 5102-5107, 2015.

[36] X. Z. Lai, Z. M. Xie, and X. L. Cen, "Design of dual circularly polarized antenna with high isolation for RFID

application," *Progress In Electromagnetics Research B*, vol. 139, pp. 25-39, 2013.
[37] X. Li, X. W. Shi, W. Hu, P. Fei, and J. F. Yu, "Compact triband ACS-Fed monopole antenna employing open-ended slots for wireless communication," *IEEE Antennas and Wireless Propagation Letters*, vol. 12, pp. 388-391, 2013.
[38] A. Boukarkar, X. Q. Lin, Y. Jiang, and Y. Q. Yu, "Miniaturized single-feed multiband patch antennas," *IEEE Transactions on Antennas and Propagation*, vol. 65, pp. 850-854, 2017.
[39] K. Wu, P. Burasa, T. Djerafi, and N. Constantin, "Millimeter-wave identification for future sensing, tracking, positioning and communicating systems," in *Proc. Global Symposium on Millimeter Waves (GSMM) & ESA Workshop on Millimeter-Wave Technology and Applications*, Espoo, 2016, pp. 1-4.

Nayan Sarker received the B.Sc. in electronics and communication engineering (ECE) degree from Khulna University of Engineering and Technology (KUET), Khulna, Bangladesh in October, 2014. Currently, he is pursuing M.Sc. engineering degree at the Institute of Information and Communication Technology (IICT) in Bangladesh University of Engineering and Technology (BUET), Dhaka, Bangladesh. He is also working as a lecturer at Bangladesh University of Business and Technology (BUBT), Dhaka, Bangladesh. His research interest is antenna design for active and passive RFID systems, IOT, OFDM and signal security.

Md. Aminul Islam (S'11, M'15) received the B.Sc. degree in electrical and electronic engineering from Bangladesh University of Engineering and Technology (BUET), Dhaka, Bangladesh, in October 2009, and the Ph.D. degree from Monash University, Clayton, Victoria, Australia, in October 2014. He worked as a Research Support Officer at Monash Microwave, Antennas, RFID, and Sensor (MMARS) laboratory in 2014–2015. Currently, he is working as an Assistant Professor at the Military Institute of Science and Technology (MIST), Bangladesh. His research interest is in chipless RFID tag, reader, and antenna designing.

M. Rubaiyat Hossain Mondal received the B.Sc. and M.Sc. degrees in electrical and electronic engineering from Bangladesh University of Engineering and Technology (BUET), Dhaka, Bangladesh in 2004 and 2007, respectively. He obtained the Ph.D. degree in 2014 from the Department of Electrical and Computer Systems Engineering, Monash University, Melbourne, Australia. From 2005 to 2010, and from 2014 to date he has been working as a Faculty Member at the Institute of Information and Communication Technology (IICT) in BUET. His research interests include wireless communications, optical wireless communications, OFDM, image processing and machine learning.